Quantum walk analyses of the off-shell scientific features of dressed-photon–phonon transfers among a small number of nanometer-sized particles

Off-shell: 10.14939/2407O.001.v1

M. Ohtsu[1], E. Segawa[2], K. Yuki[3], and S. Saito[4]

[1]Research Origin for Dressed Photon,3-13-19 Moriya-cho, Kanagawa-ku, Yokohama, Kanagawa 221-0022, Japan
[2]Yokohama National University, 79-8 Tokiwadai, Hodogaya-ku, Yokohama, Kanagawa 240-8501, Japan
[3]Middenii, 3-3-13 Nishi-shinjuku, Sinjuku-ku, Tokyo 160-0023, Japan
[4]Kogakuin University, 2665-1, Nakano-machi, Hachioji, Tokyo 192-0015, Japan

Abstract

This paper reports the results of numerical calculation of the output signal intensity emitted from a nanometer-sized particle (NP) located at the center of the surrounding NPs. A blown-up quantum walk model is used for these calculations. When the number of these NPs is as small as 4–6, the output signal intensity shows a drastic increase. This increasing feature agrees with the experimental results and implies that the dressed-photon–phonon autonomously transfers in a microscopic system composed of a small number of NPs, which is a typical off-shell scientific phenomenon.

1. Introduction

A dressed photon (DP) is a quantum field created by the interaction between photons and electrons (or excitons) in a nanometer-sized particle (NP) under light irradiation. The created DP localizes at the NP. It is an off-shell quantum field because its momentum has large uncertainty due to its subwavelength size [1, 2].

Since the DP creation originates from the light–matter interaction in a microscopic space, a spacelike momentum field must be introduced into the electromagnetic field theory. This has recently been successful in off-shell science, allowing physical pictures of the creation process to be drawn. These successful pictures have revealed the following [3,4]:

(1) A microscopic material field (a timelike momentum field) interacts with a vector boson field.

(2) In addition to a stable pair of Majorana fermions (a spacelike momentum field), an unstable pair consisting of a Majorana particle and anti-particle (timelike momentum fields) is created.

(3) Although this unstable pair annihilates within a short time duration, a novel light field (a timelike momentum field) remains at the microscopic material. This is the DP.

Furthermore, the DP couples with a phonon to create a new quantum field, named a dressed-photon–phonon (DPP). The spatial behavior of the transfer of this created DPP was analyzed by using a quantum walk (QW) model [5], and the results of this analysis agreed well with experimental results [6-12]. This paper reports the results of numerical calculations that were carried out for studying the experimentally found unique features of DPP transfer among a small number of NPs.

2. Review of experimental results

This section reviews experiments conducted to improve the optical/electrical energy conversion efficiency of a silicon photodiode (Si-PD: Hamamatsu Photonics K.K., Si photodiode S2388: Active surface area 5.8 mm × 5.8 mm) [13,14]. As schematically explained by Fig. 1(a), small and large NPs (NP_S and NP_L) were used, which were made of CdSe spherical particles. Their average diameters were 2.0 nm and 2.8 nm, respectively. These NPs were dispersed in a mixed solution of toluene and an ultraviolet (UV)-curable resin. The volume density of the dispersed NPs was controlled so that the average distance between NPs was around 40 nm. Half of the Si-PD surface was spin-coated with a resin containing a mixture of NP_S and was cured by UV radiation, whereas the other half of the surface was coated with the same resin without the NP mixture. F_{DPP} and F_0 in Fig. 1(a) represent the cured resin films on the Si-PD surface with and without the NPs, respectively. After the DPP transfers from NP_S to NP_L in F_{DPP} and creates an exciton in the higher energy level of NP_L, the exciton relaxes to the lowest energy level to emit a photon. It should be noted that the energy of this photon is red-shifted* due to the relaxation of the exciton.

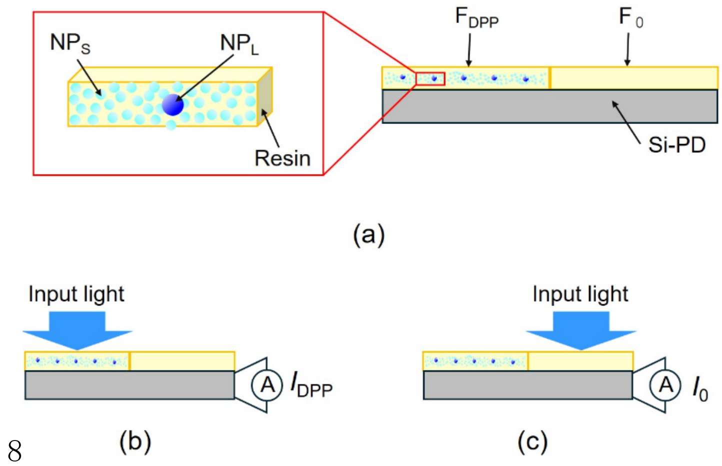

Fig. 1 A silicon photodiode on which a cured resin film is coated.

(a) Cross-sectional profile.

(b), (c) Generated photocurrents (I_{DPP} and I_0) by radiating input light onto the films F_{DPP} and F_0, respectively.

By using a deuterium lamp and a halogen lamp (wavelength: 300–400 nm) as input light sources, the photocurrents I_{DPP} and I_0, generated in the Si-PD under the films F_{DPP} and F_0, respectively, were measured. Since the Si-PD is sensitive to visible light, the photocurrent I_{DPP} (Fig. 1(b)) is larger than I_0 (Fig. 1(c)). The rate of increase of the photocurrent is defined by

$$\Delta\eta \equiv \left(I_{\mathrm{DPP}} - I_0\right)/I_0 \, . \tag{1}$$

Figure 2 shows the measured value of $\Delta\eta$ [13,14], which shows that $\Delta\eta$ is larger than 10 % when the ratio $n\left(=n_{\mathrm{S}}/n_L\right)$ between the numbers n_{S} and n_L of NP_S and NP_L is in the range of 2–6. This drastic increase and the unique dependence on n are typical off-shell scientific phenomena that have never been observed in the case of conventional on-shell scientific methods. The following sections analyze these phenomena by employing an off-shell scientific QW numerical calculation.

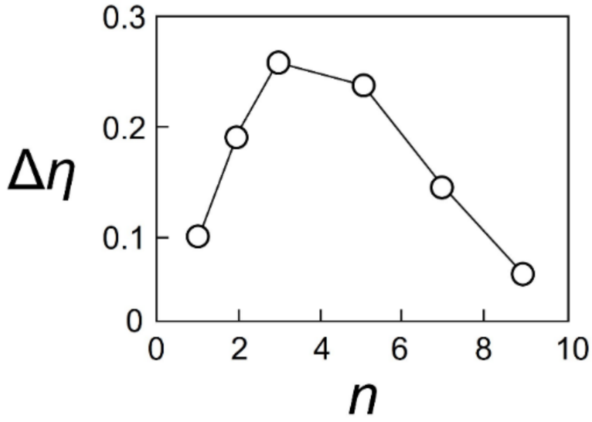

Fig. 2 Measured values of the rate of increase $\Delta\eta$ of the photocurrent.
The horizontal axis is the ratio n between the numbers of NP_S and NP_L.

(*) This is conversion from UV to visible light energy. It has been advantageously used not only to improve optical/electrical energy conversion efficiency but also to protect the Si-PD surface from deterioration induced by UV exposure [13,14].

3. A blown-up quantum walk model

This section presents a QW model for analyzing the unique features of the DPP transfer from NP_S to NP_L. Here, the optical/electrical energy conversion process in Fig. 1 does not have to be included in this model because this conversion occurs after the DPP transfer completes.

Figure 3 schematically explains how to apply the incident light (input signal) to F_{DPP} in Fig. 1 and generate the emitted light (output signal). The DPP transfer in the three-dimensional F_{DPP} is modelled by two-dimensional arrangements of NP_S and NP_L in Fig. 4, in which n NP_S (white circles ○) are arranged around one NP_L (gray circle ●). A DPP is created at these NP_Ss by light irradiation (an input signal) and transfers to the NP_L. Since the different-sized NP_S and NP_L were used in the experiment only to allow the exciton to relax to the lowest energy level of NP_L and since the relaxation process is unrelated to the DPP transfer from NP_S to NP_L, this size difference does not have to be considered in the present QW model.

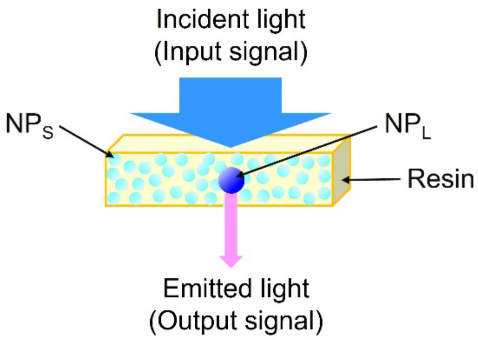

Fig. 3 How to apply the incident light (input signal) to F_{DPP} and generate the emitted light (output signal).

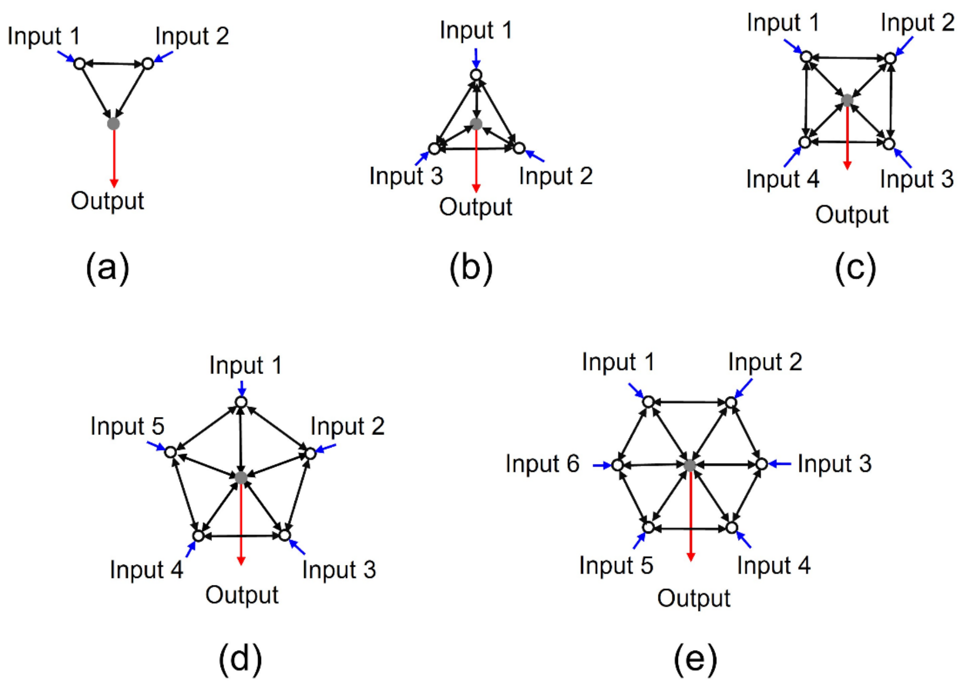

Fig. 4 Two-dimensional arrangements of NP_S and NP_L.

They are represented by white circles (◯) and a gray circle (⬤), respectively.

(a)-(e) are for $n = 2 - 6$.

The two-dimensional QW model of the arrangements in Fig. 4 has been formulated for calculating the intensity of a generated output signal [15]. In this model, in the case of Fig. 4(c) ($n = 4$), as an example, the sites for four input signals (white circles ◯) are blown up, and four internal sites are attached. They are represented by small black circles on the circumferences of the white circles in Fig. 5. These attachments are to establish routes of transfer in and out of the DPP (represented by a pair of curved arrows). These internal sites are also attached to the blown-up site for the output signal (gray circle ⬤ in Fig. 5). Finally, a side cycle (a closed loop represented by an

∞-shaped thick gray curve in Fig. 5) is selected to identify the DPP transfer route that passes through both the internal sites for input and output signals. Such internal sites and side cycle are attached also to the arrangements in Figs. 4(a), (b), (d), and (e). Their details are described in Ref. [15].

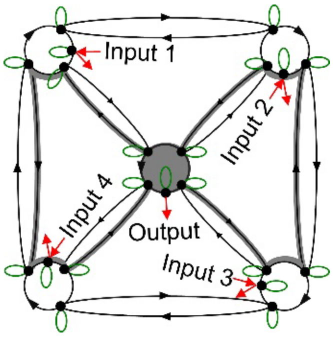

Fig. 5 Schematic explanation of a blown-up quantum walk model.

Internal sites are represented by small black circles on the circumferences of the four white circles and a gray circle. The closed loop is a side cycle that is represented by an ∞-shaped thick gray curve.

In order to represent the experimentally observed phenomenon of photon breeding with respect to photon momentum [10], it is assumed that the DP-phonon coupling constant χ [5] takes different values for the DP that hops along the directions parallel (χ_1) and anti-parallel (χ_2) to that of the incident light propagation. That is, the possibility of photon breeding occurring is assumed to be higher in the case of $\chi_1 > \chi_2$ than that of $\chi_1 < \chi_2$. The difference between these constants is represented by introducing a parameter ε into

$$\chi_1 / \chi_2 = \sqrt{(1+\varepsilon)/(1-\varepsilon)} \,. \tag{2}$$

For comparing with the case of $\chi_1 < \chi_2$, the value of ε is allowed to vary in the range of

$$-1 < \varepsilon < 1 \,. \tag{3}$$

From the QW model constructed above, Ref. [15] derived the stationary value P_{OS} of the output signal intensity, which was the value realized a sufficiently long time after the input signal was applied (refer to Fig. 10(a) in Section 5). The results demonstrated the following unique off-shell scientific features of the DPP transfer:

(1) P_{OS} increases with increasing n and asymptotically approaches $(1+\varepsilon)^2$.

(2) P_{OS} is 1 at $n = 2$, which is independent of ε.

(3) P_{OS} for $n = 3$ is equal to that for $n = 6$.

(4) P_{OS} is 1 in the case of $\varepsilon = 0$, which is independent of n.

(5) P_{OS} is independent of χ / J, where J is the hopping energy of the DP [5].

4. Results of numerical calculations

Numerical calculations were carried out by referring to the theoretical results (1)–(5) in Section 3. Figure 6 shows the calculated relation between $n(=2\text{-}12)$ and P_{OS}. Here, the value χ/J was fixed at 1 by referring to (5) in Section 3. Figs. 6(a)-(c) and (e)-(g) are the relations for $\varepsilon > 0$ ($\chi_1 > \chi_2$) and for $\varepsilon < 0$ ($\chi_1 < \chi_2$), respectively. Figure 6(d) is for $\varepsilon = 0$ ($\chi_1 = \chi_2$).

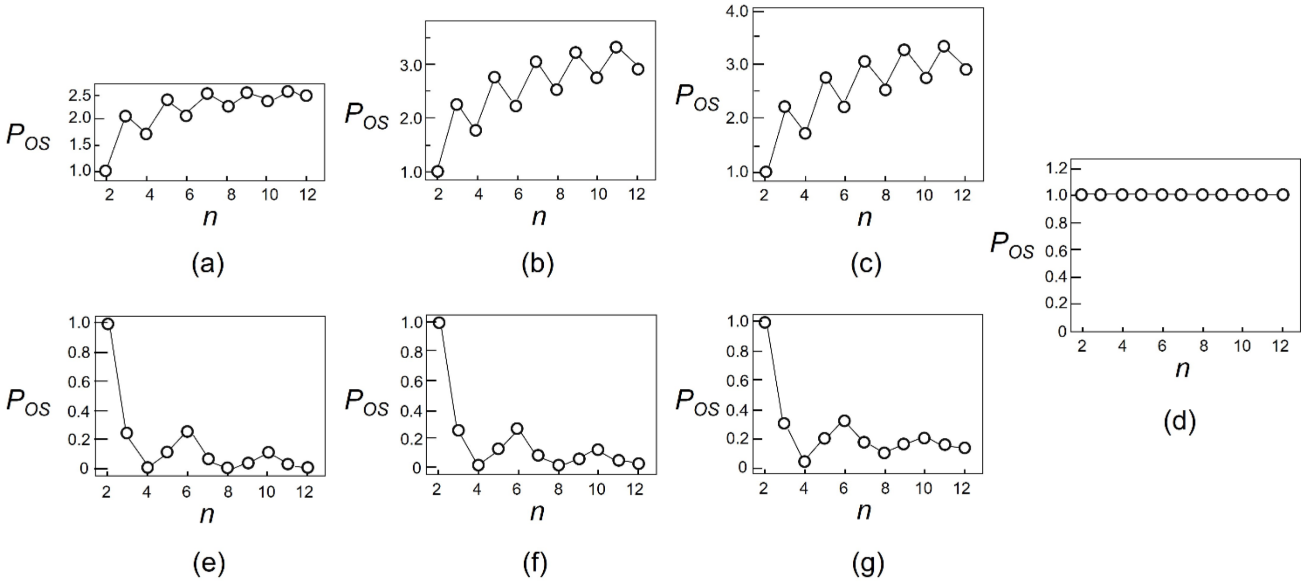

Fig. 6 Calculated relation between n and P_{OS}.
The value χ/J was fixed at 1.

(a)-(c) ε=0.600, 0.923, and 0.981 (χ_1/χ_2 =2, 5, and 10). (d) $\varepsilon = 0$ (χ_1/χ_2 =1).

(e)-(g) ε=-0.981, -0.923, and -0.600 (χ_1/χ_2 =0.1, 0.2, and 0.5).

Figure 7 shows the relation between χ_1/χ_2 in Eq. (2) and S_n. Here, S_6 and S_{12} are the sums of P_{OS} in Fig. 6 over $n = 2\text{-}6$ and $n = 2\text{-}12$, respectively. This figure indicates that the value S_n is small when $\chi_1/\chi_2 < 1$. However, it increases rapidly with increasing χ_1/χ_2 when $\chi_1/\chi_2 > 1$. As a result, S_n takes a large value in the case of $\chi_1 > \chi_2$. This result agrees with the experimental result for photon breeding with respect to photon momentum.

In Figs. 6(a)-(c), P_{OS} increases with increasing n while varying in a pulsatory manner, as schematically explained by the broken curve and white circles in Fig. 8(a), respectively. (For comparison, Figs. 6(e)-(g) show that P_{OS} decreases with pulsatory variations, as explained by Fig. 8(b).) Increases in Figs. 6(a)-(c) and Fig. 8(a) represent the typical on-shell scientific feature because

P_{OS} often increases with increasing number of NPs in a macroscopic-sized system composed of a large number of NPs. In contrast, the pulsatory variation, which is conspicuously seen in the case of a small number n, is the off-shell scientific feature of the microscopic-sized system. In order to analyze this pulsatory feature, the magnitude of deviation of the white circle from the broken curve in Fig. 8(a) is defined by

$$\Delta p_{\mathrm{OS}}(n) \equiv \frac{|P_{\mathrm{OS}}(n) - P_{\mathrm{OS}}(n-1)|}{P_{\mathrm{OS}}(n) + P_{\mathrm{OS}}(n-1)}. \tag{4}$$

Figure 9(a) is the calculated result for $\varepsilon > 0$. It shows that $\Delta p_{\mathrm{OS}}(n)$ takes a large value in the range of $n = 4$ - 6, which agrees with the experimental results in Fig. 2, and thus, the correlation with photon breeding with respect to photon momentum is confirmed*. For comparison, Fig. 9(b) shows the results for $\varepsilon < 0$, in which the value of $\Delta p_{\mathrm{OS}}(n)$ shows a complicated dependency on n. Especially for $\varepsilon = -0.981$, it takes large values at n=4, 5, 8, 9, and 12. It originates from very small values of P_{OS} (Figs. 6(a)-(c) and 7) due to the low probability of photon breeding occurring.

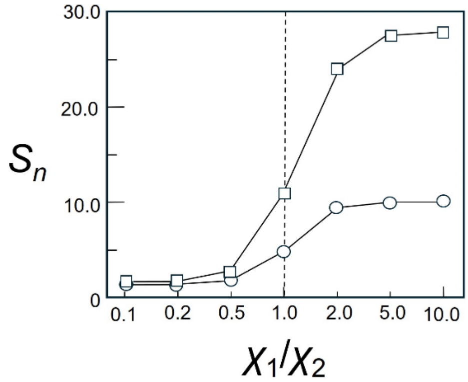

Fig. 7 Relation between χ_1/χ_2 and S_n.
S_6 and S_{12} are the sums of P_{OS} in Fig. 6 over $n = 2$ - 6 and $n = 2$ - 12, respectively.

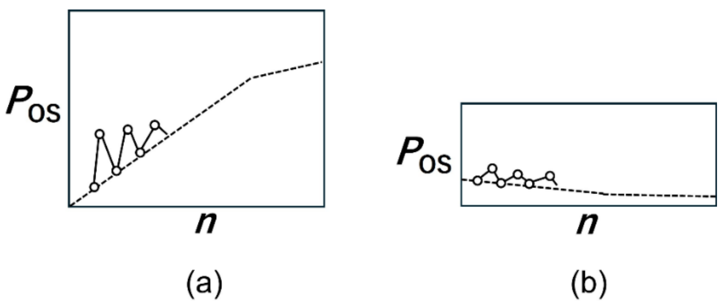

Fig. 8 Schematic explanation of the variations (broken curves) of P_{OS} and pulsatory deviation (white circles) from the broken curves.
(a) and (b) are for the case of $\varepsilon > 0$ and $\varepsilon < 0$, respectively.

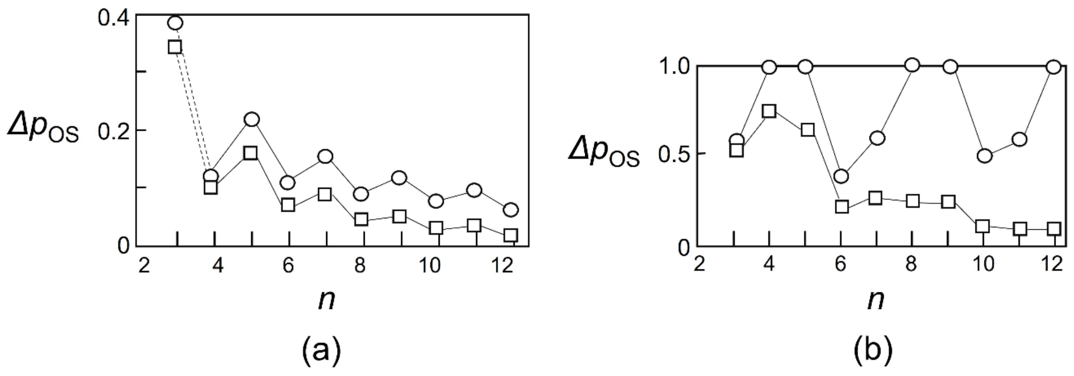

Fig. 9 Relation between n and $\Delta p_{\mathrm{OS}}(n)$.

(a) For the case of $\varepsilon > 0$. White circles and squares are for ε=+0.981 and +0.600, respectively.

(b) For the case of $\varepsilon < 0$. White circles and squares are for ε=-0.981 and -0.600, respectively.

(*) Figure 9(a) shows that $\Delta p_{\mathrm{OS}}(n)$ takes a distinctly large value at $n = 3$. Since it originates from feature (2) in Section 3, further studies on the QW model are required to explore this origin.

---

5. Discussion

In Fig. 9(a), large values of $\Delta p_{\mathrm{OS}}(n)$ in the range $n = 4$ - 6 imply that the phenomena occurring in a microscopic system composed of a small number n are very different from those in a macroscopic system. Although the macroscopic phenomena follow the popular on-shell scientific principle of least action, the large values in Fig. 9(a) mean that the DPP in the microscopic system is free from this principle and can transfer in an autonomous manner. Such autonomous transfer has been implied by a variety of experimental results on DPPs, including the experimental results in Fig. 2 [11].

In further studies on the autonomous transfer, it could be advantageous to analyze the temporal variation of the output signal intensity $P_{\mathrm{O}}(t)$ in the transient time period that starts immediately after the input signal is applied to the system. Figure 10(a) shows the profile of $P_{\mathrm{O}}(t)$. Figures 10(b) and (c) show the calculated time t_{s} required to converge to the stationary value P_{OS} for $\varepsilon > 0$ and for $\varepsilon < 0$, respectively. This time t_{s} depends on n for $\varepsilon > 0$ (Fig. 10(b)). In contrast, it is independent of n for $\varepsilon < 0$ (Fig. 10(c)). Calculations also found that the time t_{s} depended on the value of χ/J, which is different from feature (5) in Section 3.

Furthermore, within the transient time period ($t < t_{\mathrm{S}}$), $P_{\mathrm{O}}(t)$ pulsates in the case of $\varepsilon > 0$, and can take a larger value (white square in Fig. 10(a)) than P_{OS}. This pulsatory variation feature implies that the DPP tries to find the transfer routes in Fig. 5 in a unique manner to autonomously fix the optimum route to the $\mathrm{NP_L}$. To investigate this further, temporal variations of the DPP creation probabilities should be evaluated more quantitatively, not only for the output terminal $\mathrm{NP_L}$ but also for each NP_S.

Since the positions and sizes of NP_S and NP_L can fluctuate when they are dispersed in the UV-curable resin in Fig. 1(a) [16], the QW model in Figs. 4 and 5 should be slightly modified by taking these fluctuations into account. Furthermore, it may be advantageous to replace the two-dimensional model in Fig. 4 by a three-dimensional one [10]. More accurate comparisons between calculated and experimental results are expected by doing so.

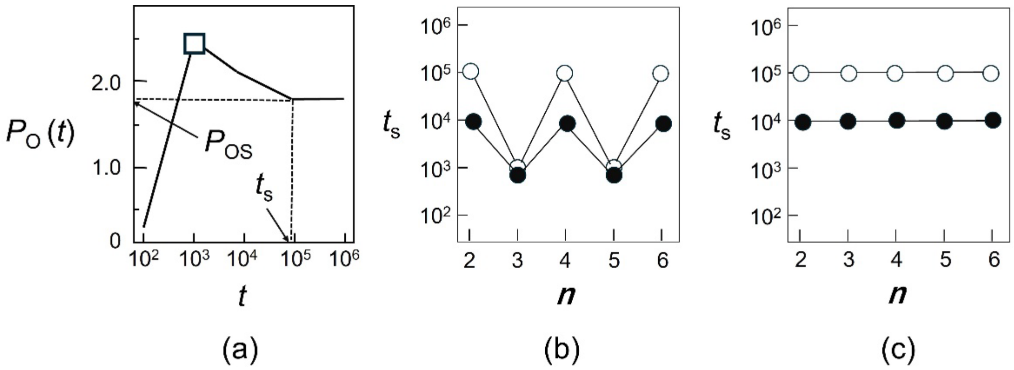

Fig. 10 Temporal variation of the output signal intensity $P_O(t)$.

(a) Profile of $P_O(t)$ for n=5 and ε=+0.981. t_s represents the time required to converge to the stationary value P_{OS}. The white square represents the value at the peak of the pulsatory variation, which is larger than P_{OS}.

(b) For the case of $\varepsilon > 0$. White and black circles are for ε=+0.981 and +0.923, respectively.

(c) For the case of $\varepsilon < 0$. White and black circles are for ε=-0.981 and -0.923, respectively.

6. Summary

This paper reported the results of numerical calculations of the output signal intensity emitted from a nanometer-sized particle (NP: output terminal), which was located at the center of surrounding NPs (input terminals). A blown-up quantum walk model was used for these calculations, and the results indicated that the output intensity increased with increasing number of surrounding NPs. However, when this number was as small as 4–6, the intensity deviated from this trend and showed a drastic increase. This agreed with the experimental results. This deviation implied that the DPP autonomously transferred in a microscopic system composed of a small number of NPs, which is a typical off-shell scientific phenomenon.

References

[1] M. Ohtsu, I. Ojima, and H. Sakuma, "Dressed Photon as an Off-Shell Quantum Field," Progress in Optics Vol.64, (ed. T.D. Visser) pp.45-97 (Elsevier, 2019).

[2] M. Ohtsu, , *Off-Shell Applications In Nanophotonics*, Elsevier, Amsterdam (2021) p.5.

[3] H. Sakuma, I. Ojima, M. Ohtsu, and T. Kawazoe, Drastic advancement in nanophotonics achieved by a new dressed photon study, "JEOS-RP (2021) **17**: 28.

[4] H. Sakuma, I. Ojima, and M. Ohtsu, “Perspective on an Emerging Frontier of Nanoscience Opened up by Dressed Photon Studies,” *Nanoarchitectonics*, Vol. 5, Issue 1 (2024) pp.1-23.
[5] M. Ohtsu, “A Quantum Walk Model for Describing the Energy Transfer of a Dressed Photon,” *Off-shell Archive* (September, 2021) OffShell: 2109R.001.v1.
DOI 10.14939/2109R.001.v1, http://offshell.rodrep.org/?p=345
[6] M. Ohtsu, E. Segawa, and K. Yuki, “Numerical calculation of a dressed photon energy transfer based on a quantum walk model,” *Off-shell Archive* (June, 2022) OffShell: 2206O.001.v1.
DOI 10.14939/2206O.001.v1
https://rodrep.or.jp/en/off-shell/original_2206O.001.v1.html
[7] M. Ohtsu, E. Segawa, K. Yuki, and S. Saito, “Dressed-photon—phonon creation probability on the tip of a fiber probe calculated by a quantum walk model,” *Off-shell Archive* (December, 2022) OffShell: 2212O.001.v1.
DOI 10.14939/2212O.001.v1
https://rodrep.or.jp/en/off-shell/original_2212O.001.v1.html
[8] M. Ohtsu, E. Segawa, K. Yuki, and S. Saito, “Spatial distribution of dressed-photon–phonon confined by an impurity atom-pair in a crystal,” *Off-shell Archive* (January, 2023) Offshell: 2301O.001.v1.
DOI 10.14939/2301O.001.v1
https://rodrep.or.jp/en/off-shell/original_2301O.001.v1.html
[9] M. Ohtsu, E. Segawa, K. Yuki, and S. Saito, “A quantum walk model with energy dissipation for a dressed-photon–phonon confined by an impurity atom-pair in a crystal,” *Off-shell Archive* (April, 2023) Offshell: 2304O.001.v1.
DOI 10.14939/2304O.001.v1
https://rodrep.or.jp/en/off-shell/original_2304O.001.v1.html
[10] M. Ohtsu, E. Segawa, K. Yuki, and S. Saito, “Analyses of photon breeding with respect to photon spin by using a three-dimensional quantum walk model,” *Off-shell Archive* (November, 2023) Offshell: 2311O.001.v1.
DOI 10.14939/2311O.001.v1
https://rodrep.or.jp/en/off-shell/original_2311O.001.v1.html
[11] M.Ohtsu "Off-shell scientific nature of dressed photon energy transfer and dissipation," Offshell: 2404R.001.v1.
DOI 10.14939/2404R.001.v1
https://rodrep.or.jp/en/off-shell/review_2404R.001.v1.html
[12] M.Ohtsu, E.Segawa, K.Yuki, and S.Saito "Optimum dissipation for governing the autonomous transfer of dressed photons," Offshell: 2405O.oo1.v1.
DOI 10.14939/2405O.001.v1
https://rodrep.or.jp/en/off-shell/original_2405O.001.v1.html
[13] M. Naruse, T. Kawazoe, R. Ohta, W. Nomura, M. Ohtsu, "Optimal mixture of randomly dispersed quantum dots for optical excitation transfer via optical near-field interactions," Phys. Rev. B **80**, 125325 (2009)
[14] M. Naruse, K. Leibnitz, F. Peper, N. Tate, W. Nomura, T. Kawazoe, M. Murata, M. Ohtsu, “Autonomy in excitation transfer via optical near-field interactions and its implications for information networking,” Nano Commun. Networks **2**, (2011) pp. 189-195.
[15] E. Segawa, S. Saito, K. Yuki, M. Ohtsu, "Paths on the graph chosen autonomously by dressed photons from the

quantum walk model, " Abstracts of the 85th Jpn. Soc. Appl. Phys. Autumn Meeting, (September 16-20, 2024) (Toki Messe, Niigata) paper number 18p-A33-18. To be presented (in Japanese).
[16] W. Nomura, T. Yatsui, T. Kawazoe, M. Naruse, and M. Ohtsu, "Structural dependence of optical excitation transfer via optical near-field interactions between semiconductor quantum dots," Appl. Phys. - Lasers and Optics, Vol. 100, July 2010, pp.181-187.